ADSORPTION OF STREPTAVIDIN ONTO POLYSTYRENE SURFACE

Department of Physical Chemistry
Faculty of Science, Lund University
SE-221 00, Lund, Sweden

LUND UNIVERSITY

Author:
Lina Le

Supervisors:
Peter Jönsson
Mohammad Arif Kamal

Examiner:
Viveka Alfredsson

MARCH 1, 2018

Abstract

Microparticles of various sizes carrying different surface modifications have numerous technological and biomedical applications, for example to create a larger target for a molecular receptor by binding multiply ligands to the surface of the microparticle. The aim of the present work is to study how to most efficiently couple protein molecules to the surface of such microparticles. In the current study I have focused on the coupling of Streptavidin-Alexa Flour 488 (SA-AF 488) to polystyrene microparticles (PSMs). The passive adsorption of SA-AF 488 onto PSMs with diameter 6 µm was first investigated at two different pH. It was found that maximal adsorption occurs when pH is in the neighbourhood of SA-AF's isoelectric point. However, the protein adsorption on the PSMs was uneven for the passive adsorption. To obtain a more even protein adsorption I then investigated covalent coupling of the same protein on carboxyl-modified PSMs (PSM-COOH) as well as amine modified PSMs (PSM-NH_2) with diameter 1 µm. This approach resulted in more even protein coverage on the PSMs and of the two covalently-coupled PSMs it was found that the PSM-COOH bound more proteins in comparison to PSM-NH_2. The study shows that efficiently coupling of protein molecules can be achieved to microparticles, opening up for different proteins such as antibodies to be coupled to microspheres of various sizes.

Contents

POPULÄRVETENTENSKAP ..... ERROR! BOOKMARK NOT DEFINED.

ABSTRACT I

CONTENTS II

1. INTRODUCTION 1

1.1 BACKGROUND AND MOTIVATION 1

1.2 PROJECT DESCRIPTION 1

1.3 OUTLINE OF THE REPORT 2

2. BACKGROUND 4

2.1 PROTEIN COUPLING TO MICRO- AND NANOPARTICLES 4

2.2 COLLOIDAL STABILITY 5

3. EXPERIMENTAL METHODS 7

3.1 COUPLING OF PROTEINS TO MICROSPHERES 7

3.1.1 PASSIVE ADSORPTION 7

3.1.2 COVALENT COUPLING 7

3.1.2.1 Mechanism *7*

3.1.2.2 Procedure *11*

3.2 CENTRIFUGATION 12

3.3 NANODROP 14

3.3.1 BASICS OF NANODROP 14

3.3.2 BEER-LAMBERT'S LAW 14

3.3.3 PRINCIPLE OF A280 MEASUREMENT AND DETERMINATION OF PROTEIN CONCENTRATION 15

3.4 MICROSCOPY 15

3.4.1 BASIC OF LIGHT MICROSCOPY 15

3.4.1 FLUORESCENCE MICROSCOPY 16

3.4.2 CONFOCAL MICROSCOPY 17

4. RESULTS AND DISCUSSION 19

4. PASSIVE ADSORPTION 19

4.2 COVALENT COUPLING 24

4.2.1 Amino-modified PSMs (PSM-NH2) *24*

4.2.2 Carboxylate -modified PSM (PSM-COOH) *28*

5. CONCLUSION 32

5.1 CONCLUSION 32
5.2 FUTURE WORK 32
6. ACKNOWLEDGEMENTS 33
REFERENCES 34
APPENDIX 38
SOURCE CODE 38
Calculations for Polystyrene microparticle 38
Calculations for Streptavidin 39

Chapter 1

1. Introduction

1.1 Background and Motivation

In biomedical field, the protein adsorbed polystyrene (PS) latex particle are widely used in diagnosis of Chagas disease and cancer, application in white blood cell counting, and effort in the field of biosensor [1]. For the application to the solid-phase immunodiagnostic assay, protein-PS conjugate must be stable until the immunological reaction is complete and the absorbed protein on the surface must have homogenous distribution [2]. Protein adsorption to the PS surface is known to be achieved in many ways such as Van der Waals forces, hydrogen bonding, and electrostatic as well as hydrophobic forces [3]. Passive adsorption allows the physical interaction between protein and surface of PS particles in aqueous solution by hydrophobic forces [3] [4] [5] while covalent coupling is a result of electrostatic interaction which allows the binding of protein to PS particle via surface modification [6] [5]. Covalent adsorption onto polystyrene surface is processed by functionally modified reactive groups such as aldehyde, amino, carboxyl, hydroxyl, and sulphate [7].

Protein adsorption to the PS surface is interested because the same protocol can be used to couple polystyrene nanoparticles in order to increase the size of antibody. Thereafter, the antibody-conjugated nanoparticles are transferred to the T-cells for further study such as hydrodynamic trapping.

1.2 Project Description

The aim with this master's thesis was to study how to efficiently couple proteins to microparticles. As a model system I used polystyrene microspheres (PSMs) of size 1 and 6 μm. The polystyrene chain is a linear hydrocarbon chain with a benzene ring attached to every second carbon atom. The aromatic rings regulate how the chain coils and entangle (see Figure 1). The surface is hydrophobic in character [8].

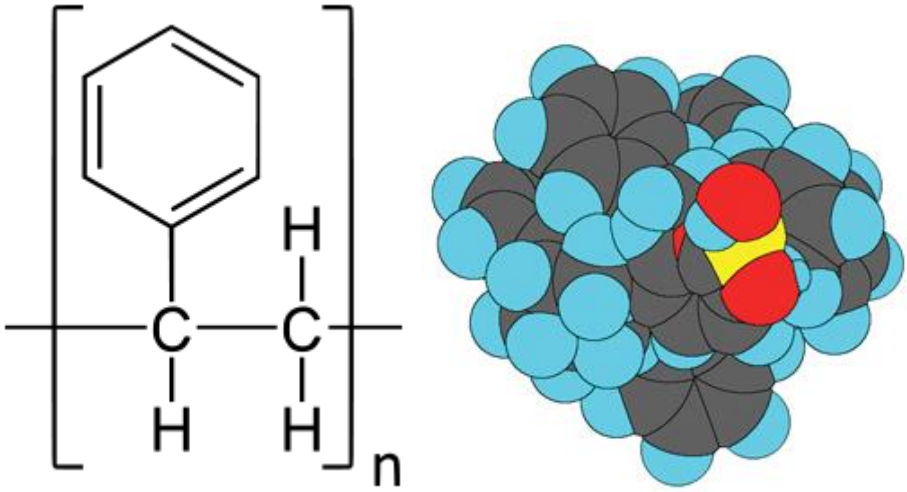

Figure 1 [8]. (Left) Repeating unit of polystyrene chain. (Right) This figure shows a section of the surface of a PSM that are stabilized against aggregation by covalently linked charge groups. The view looks down onto the surface above a sulphate group (red and yellow). The benzene rings (grey area) dominate the field and present a markedly hydrophobic surface ideal for the adsorption of proteins.

The protein to be bound to the PSMs was streptavidin-Alexa Fluor 488 (SA-AF 488). Streptavidin is a biotin-binding protein with an isoelectric point of 5. The molecular weight is 52.8 kDA and the protein is composed of 4 essentially identical polypeptide chains.

The thesis contains a detailed description of the experimental steps to couple the proteins to the polystyrene microparticles, a quantitative as well as qualitative analyses of the protein-polystyrene microspheres and a discussion of how to most efficiently couple proteins to microparticles based on this.

1.3 Outline of the report

This master's thesis starts with a review of protein coupling to micro- and nanoparticles and the theory of colloidal stability in Chapter 2. Chapter 3 explains the methodology used, as well as how to couple protein to microspheres. In Chapter 4 the results are discussed and analysed. Finally, Chapter 5 draws conclusions and summarizes the report.

Chapter 2

2. Background

2.1 Protein coupling to micro- and nanoparticles

Recently, nanoparticles have become popular for biomedical application because they are tuneable, functionable and biocompatible vehicles that can be used for transportation of objects at higher concentrations than traditional methods [9]. The surface of nanoparticles can be modified with high affinity disease-specific targeting ligands to enhance selective transportation. Many chemical and biological molecules such as small molecules, sugars, fatty acids, proteins, peptides, antibodies, and aptamers have been studied to improve the targeting purposes [10].

The structure of the nanoparticle is important. The nanoparticle must be biologically inert, stable under physiological conditions, move freely, safely capture chemical objects, and easily be coupled to the targeting molecule. A popular coupled protein is antibodies. Antibodies operate by aiming specific antigens. Because antigens locate mainly on the surface of diseased cell, antibodies can theoretically be used to carry nanoparticles through the body and enable selective delivery. In early developments, only full antibodies were used as targeting ligand. However, the usage of full antibodies had several problems such as immunogenicity [11], fast elimination [12], poor stability [13], and low efficacy [9]. Antibody fragments appear to improve efficacy as they are less immunogenic. In addition to being less immunogenic, the smaller size of antibody fragments increases the loading capacities and superior orientation of targeting ligands [10]. When antibody fragment conjugates to the nanoparticle, it should happen in a way such that the shape, size, and functionality of both the nanoparticle and the antibody fragment are negligibly affected.

Nanoparticle surface modification can be divided into two main groups: covalent and non-covalent. In covalent modifications, a ligand is covalently attached to a chemically-functionalized group. In non-covalent modification, a ligand interacts non-

specifically with the surface by different intermolecular forces (electrostatic, van der Waals forces, hydrophobicity…). Covalent methods are preferred for coating nanoparticles with antibodies as they give better stability. Besides, the position and orientation of attached antibody fragments can be controlled with covalent methods.

2.2 Colloidal Stability

A colloidal particle has Brownian motion in solution. It can interact not only with solvent molecules but also with other colloidal particles, which if the latter interactions are attractive will result in clustering of the particles. The two main forces between charged colloidal particles in an electrolyte solution are the repulsive electrostatic double layer interaction and the attractive van der Waals (vdW) interaction. The balance of these two interactions can result in either attraction or repulsion. This is taken into consideration in the DLVO theory which can be used to explain the stability of colloidal systems. The DLVO theory assumes that behaviour of colloidal suspensions is controlled mainly by the interaction potential between two particles [14]. The potential energy of vdW interaction between two spherical particles, $V_A\ (H)$, is given by [15]:

$$\boldsymbol{V_A(H) = -\frac{A_a * a}{12H}} \quad \mathbf{1}$$

Where A is the Hamaker constant; H is the distance between the two particles, and a is the radius of the particle. The potential energy of the electrostatic double-layer interaction, V_R, is given by [15]:

$$\boldsymbol{V_R(H) = \frac{64\pi a \gamma^2 nkT}{\kappa^2} \exp(-\kappa H)} \quad \mathbf{2}$$

With

$$\boldsymbol{\kappa = \sqrt{\frac{2nz^2e^2}{\varepsilon_r \varepsilon_0 kT}}} \quad \mathbf{3}$$

$$\boldsymbol{\gamma = \frac{exp(ze\psi_0/2kT) - 1}{exp(ze\psi_0/2kT) + 1}} \quad \mathbf{4}$$

Where κ is the inverse Debye length, ε_r is the relative permittivity of the medium, ε_0 is the permittivity of vacuum, z is the valency of the electrolyte ions, n is the bulk

electrolyte concentration, *k* is the Boltzmann constant, *T* is the temperature and ψ_0 the surface potential of the particles. The total potential energy of the interaction between the two particles, $V_T(H)$, is the sum of the vdW and the electrostatic interaction energies:

$$V_R(H) = \frac{64\pi a \gamma^2 nkT}{\kappa^2} \exp(-\kappa H) - \frac{A_a * a}{12H} \quad 5$$

A representative curve showing how the potentials vary with distance *H* is given in Figure 1.

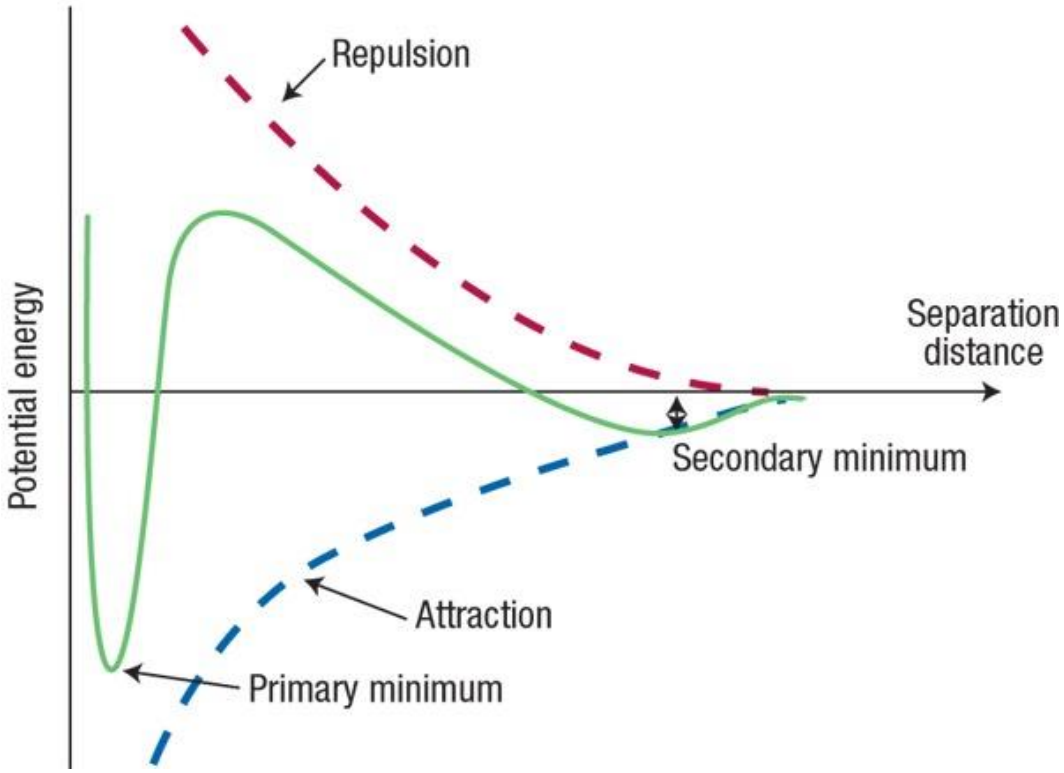

Figure 2 [16]. Interaction potential energy as a function of distance between two particles. The DLVO potential (green line) is obtained by adding electric-double layer and van der Waals potentials. The depth of the secondary minimum and the height of the DLVO potential indicate how stable the system is.

Chapter 3

3. Experimental Methods

3.1 Coupling of proteins to microspheres

3.1.1 Passive Adsorption

1. Take 50 µL of 10% w/v suspension of PSMs with 6 µm, manufactured by Bangs Laboratories, in an Eppendorf tube.
2. Add 50 µL of absorption buffer and mix. Two adsorption buffers were used: 0.1M MES pH 5 and 10mM HEPES pH 7.4
3. Centrifuge until the PSMs pellet out. In this case, the PMSs were centrifuged for 3 minutes at 523 relative centrifugal force (r.c.f).
4. Remove supernatant, resuspend the PSMs in 50 µL of absorption buffer using a pipette and then centrifuge again.
5. Repeat Steps 3 and 4, twice.
6. Add 1 µL of the 1mg/mL Streptavidin-Alexa Fluor 488 and mix gently using a pipette. Incubate overnight at 4°C.
7. Centrifuge for 5 min at 208 r.c.f and save the supernatant for determination of how much protein that has bound the PSMs.
8. Resuspend the pellet in 50 µL of storage buffer (0.1M MES pH 5 or 10mM HEPES pH 7.4). Store at 4°C.

3.1.2 Covalent Coupling

3.1.2.1 Mechanism

a. Carboxyl-modified microspheres

1-Ethyl-3-[3-dimethylaminopropyl] carbodiimide hydrochloride (EDC or EDAC) is a crosslinking agent used to couple carboxyl groups to primary amines. It causes direct conjugation of carboxylate to primary amine without becoming part of the final amide-bond. The reaction starts with the deprotonation of a carboxylic acid group of the

carboxyl-modified microspheres (Step 1). Thereafter, an active O-acylisourea intermediate is formed by nucleophilic attack from the carboxylate ion to the EDC (Step 2). The intermediate is easily displaced by the nucleophilic attack from the ligand with available amine (Step 3-5). The ligand forms an amide bond with the carboxyl-modified microsphere and an isourea which is a soluble urea derivative is released as an EDC by-product. The O-acylisourea intermediate is unstable in aqueous solutions. If the intermediate is not able to react with the primary amine, it is hydrolyzed. The carboxyls are regenerated and an N-unsubstituted urea is released.

b. Amino- modified microspheres

Aldehydes are reactive variants of carbonyl. The polarity of the carbon-oxygen double bond makes the carbon electrophilic and reactive to nucleophiles such as primary amines. In the first part of the reaction, the amino-modified microspheres react with one aldehyde group of glutaraldehyde to give an unstable addition compound called carbinolamine (Step 1-2). Since carbinolamine is an alcohol, it will undergo acid catalyzed dehydration (Step 3-4). In an acid catalysis, the Schiff base is protonated, giving the iminium ion (Step 5). The Schiff base which is formed with ordinary amines rapidly reverses in aqueous solution and therefore must be reduced to an alkylamine linkage to remain stable (Step 6). After the first reductive amination, we achieve the aldehyde–activated microspheres. To couple the ligand with available amine to the aldehyde-activated microspheres, the reductive amination is performed again to form a covalent bond between the unreacted aldehyde group of glutaraldehyde and the amine group of the ligand.

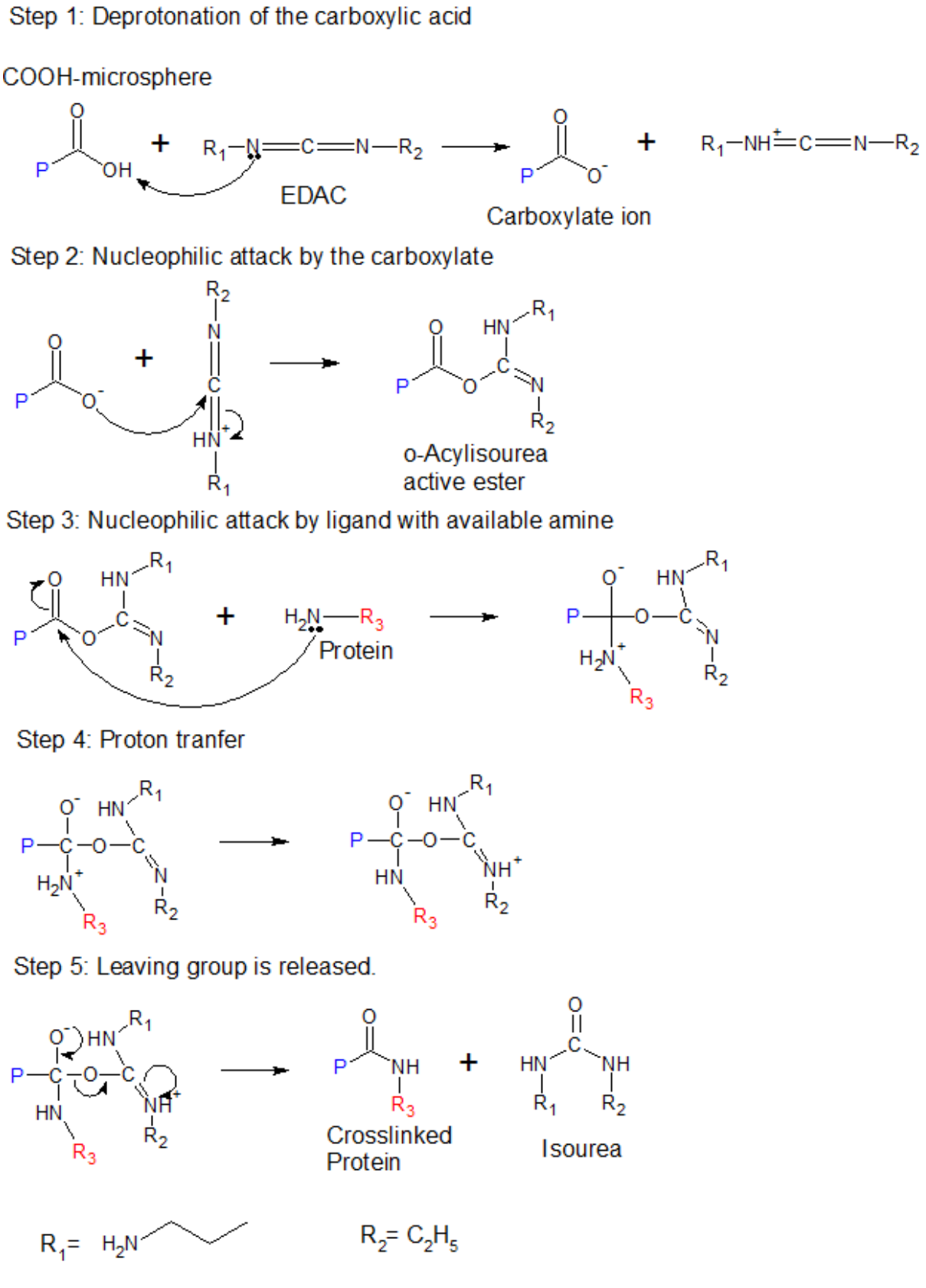

Figure 3. EDC crosslinking reaction mechanism: Carboxyl-to-amine crosslinking with carbodiimide. Molecules (P) and (R3) can be peptides, proteins or any chemicals that have respective carboxylate and primary amine groups. In this case, (P) is a microsphere and (R3) is SA-AF 488.

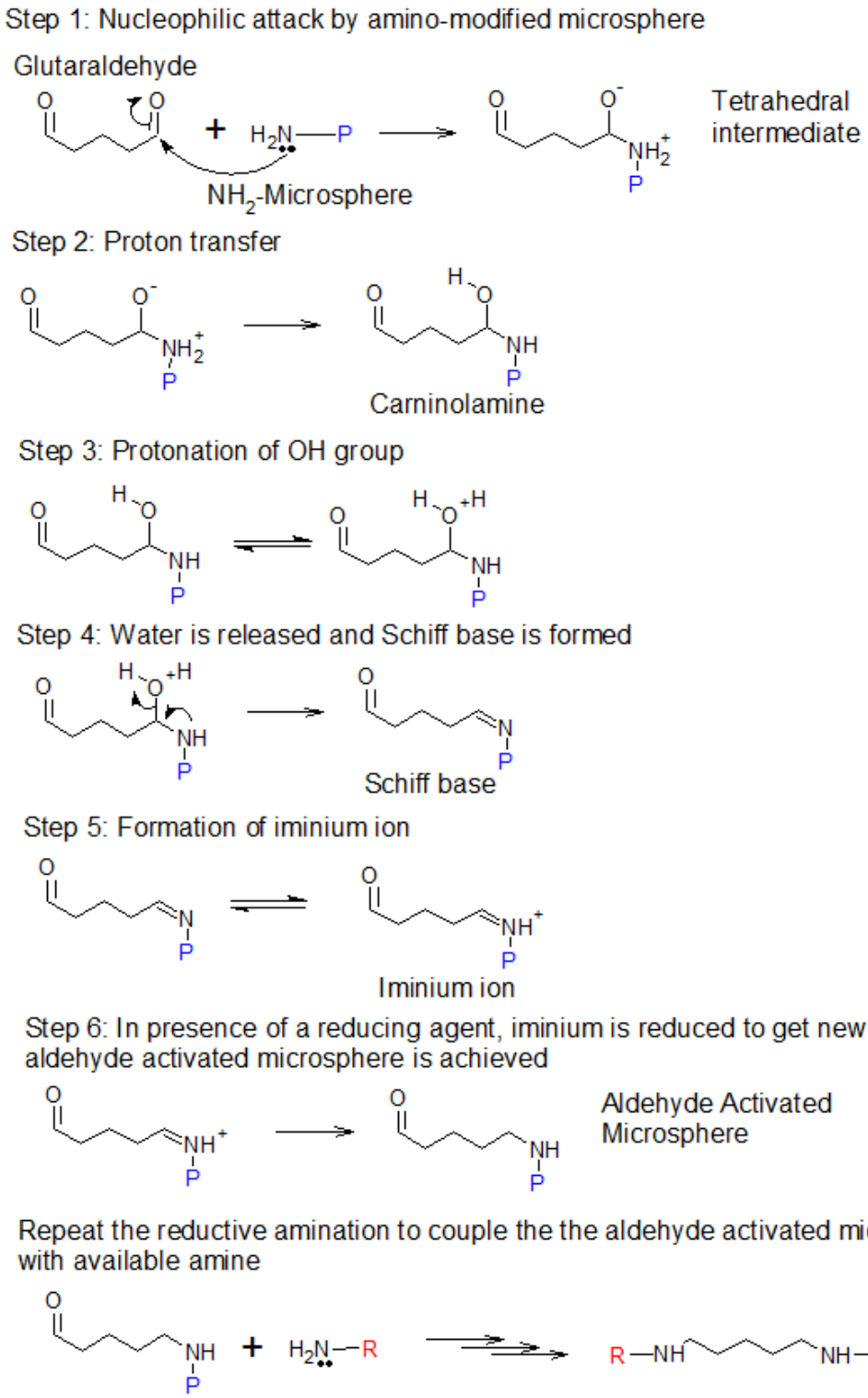

Figure 4. Reductive amination, the conjugation of the aldehyde and primary amine. In the first reductive amination, the amino-modified microspheres react with one aldehyde group of glutaraldehyde to yield the aldehyde-activated microspheres. In the second reductive amination, the aldehyde-activated microspheres will react with the remaining aldehyde group of glutaraldehyde to couple the ligands to the microspheres.

3.1.2.2 Procedure

a. Carboxyl-modified microspheres

1. Transfer 5 µL of 10% w/v suspension of PSM-COOH with 1 µm, manufactured by Bangs Laboratories, into an Eppendorf tube.
2. Add 50 µL of 0.1M MES buffer, pH 5.
3. Centrifuge for 5 minutes at 5000 r.c.f.
4. Remove and discard supernatant.
5. Repeat Step 2, 3, 4 twice.
6. After second wash, resuspend the pellet in 50 µL of 0.1M MES buffer.
7. Add 50 µL of 2% Carbodiimide in 0.1M MES pH 5.
8. Mix for 25-20 minutes at room temperature.
9. Centrifuge for 5 min at 5000 r.c.f. Remove and discard supernatant.
10. Resuspend in 0.2M Borate buffer pH 8.5.
11. Centrifuge for 5 minutes at 5000 r.c.f. Remove and discard supernatant.
12. Repeat Step 10, 11 twice to get rid of unreacted carbodiimide.
13. Resuspend in 50 µL of 0.2M Borate buffer.
14. Add 5-10 µL of 1 mg/mL Streptavidin-Alexa Fluor 488. Mix gently for 2-4 hours at room temperature.
15. Centrifuge for 10 minutes at 5000 r.c.f. Note the volume of supernatant and save for protein determination.
16. Resuspend in 0.25M Ethanolamine in 0.2M borate buffer pH 8.5. Mix gently for 30 minutes at room temperature.
17. Centrifuge for 5 min at 5000 r.c.f. Remove and discard supernatant.
18. Resuspend in storage buffer (three different storage buffers were used: 1mg/mL β-casein in PBS, 1mg/mL glycine in PBS, and PBS). Centrifuge for 5 minutes at 5000 r.c.f. Remove and discard supernatant.
19. Repeat Step 18.
20. Resuspend in 200 µL of storage buffer. Store at 4°C.

b. Amino-modified microspheres

1. Transfer 5 µL of 10% w/v of PSM-NH_2 with 1 µm, manufactured by Bangs Laboratories, into an Eppendorf tube.

2. Add 50 µL of 0.02M PBS buffer pH 7.4.
3. Centrifuge for 5 minutes at 5000 r.c.f.
4. Remove and discard supernatant.
5. Repeat Step 2, 3, 4 twice.
6. After second wash, resuspend pellet in 50 µL of 8% glutaraldehyde in 0.02M PBS buffer pH 7.4.
7. Mix gently for 2-4 hours at room temperature.
8. Centrifuge for 5 min at 5000 r.c.f. Remove and discard supernatant.
9. Wash the pellet three times with 0.02M PBS.
10. Resuspend the washed pellet in 50 µL of PBS buffer.
11. 1Add 5-10 µL of protein to couple. Mix gently for 2-4 hours at room temperature.
12. 15. Centrifuge for 10 minutes at 5000 r.c.f. Note the volume of supernatant and save for protein determination.
13. Resuspend in 0.25M Ethanolamine in 0.02 M PBS. Mix gently for 30 minutes at room temperature.
14. Centrifuge for 5 min at 5000 r.c.f. Remove and discard supernatant.
15. Resuspend in storage buffer. Centrifuge for 5 minutes at 5000 r.c.f. Remove and discard supernatant.
16. Repeat Step 15.
17. Resuspend in 200 µL of storage buffer. Store at 4°C.

3.2 Centrifugation

A centrifuge uses centrifugal force to separate particles. When a mixture is rotated at a chosen speed or revolution per minute (rpm), the centrifugal force will cause the particles to move away from the axis of rotation. The force on the particles compared to the gravity is called Relative Centrifugal Force (r.c.f). [17]

When one object travels in a circle, the force that pulls the object away from the centre of rotation is the centrifugal force. This centrifugal force is proportional to the radius, to the mass and to the square of the angular velocity [17]. It is defined by the relation:

$$\boldsymbol{F = \frac{mv^2}{r} = 4\pi^2 mn^2 r} \quad \mathbf{6}$$

Where $\boldsymbol{F}$ is the centrifugal force, m is the mass of the body, v is the velocity of the body, r is the radius of circle of rotation and n is the number of revolutions per second [18].

The separation rate by gravitational force of particles depends on particle size and density. The Stokes equation which describes movement of a sphere in gravitational field can be used to explain this sedimentation of particles [19]. The velocity of the sedimentation is:

$$\boldsymbol{V = \frac{d^2(\rho - L)3G}{18\eta}} \quad \mathbf{7}$$

d is the diameter of the spherical particle, ρ is the particle density, L is the density of the medium, η is viscosity of the medium and G is the gravitational force. From the Stokes equation, some important behaviour of particles can be concluded:

1. The sedimentation rate is proportional to the size and density of the particle.
2. The sedimentation rate is zero when the density of the particle and medium is equal.
3. The sedimentation rate decreases as the medium viscosity increases.
4. An increase in gravitational force will increase the sedimentation rate.

There are two types of centrifugation separations: differential centrifugation and density gradient centrifugation. The density gradient centrifugation can further be divided into rate-zonal and isopycnic centrifugation. The simplest centrifugal technique is differential centrifugation. In this centrifugation, particles of different size and density will sediment at different rates with the largest and most dense particles sedimenting the fastest. Differential centrifugation is usually used for collecting cells or producing subcellular fraction from tissue homogenate. In this study, differential centrifugation will be employed to wash the polystyrene microparticles.

Density gradient centrifugation is better method to purify subcellular organelles and macromolecules. Density gradient separation can be classified into two categories:

rate-zonal separation that separates particles after sizes and isopycnic separation that separates after densities.

3.3 Nanodrop

3.3.1 Basics of Nanodrop

Nanodrop technology is designed for measuring concentration of microvolume samples such as proteins, DNA, RNA, and other biomolecules. This advanced spectrophotometer uses a sample retention system that holds the sample between two optical pedestals without the uses of cuvettes or capillaries. The surface tension creates a column between the ends of two optical fibers. Thus, the measurement optical path is formed.

Removing cuvette gives many advantages: very small volume of sample is required, the optical surfaces are easily cleaned, and the path length can be varied during the measurement.

3.3.2 Beer-Lambert's Law

When a beam of light with intensity I_0 is absorbed by a sample of absorbing species, the transmitted intensity I will vary with the length, b, of the sample as well as the molar concentration of absorbing species, c, in accord with **Beer-Lambert's law**:

$$\boldsymbol{I = I_0 e^{-\varepsilon c b}} \quad \mathbf{8}$$

The quantity ε is the **molar absorption coefficient** (or extinction coefficient). The molar absorption coefficient tells how much light is absorbed at a chosen wavelength. Its dimensions are 1/ (concentration×length) [20]. The product εcb is known as the *optical density* of the sample.

Transmittance, $\boldsymbol{T}$, is the fraction of the incident intensity that passes through the sample:

$$\boldsymbol{T = \frac{I}{I_0}} \quad \mathbf{9}$$

and the absorbance, A, is defined as:

$$A = \log\left(\frac{I_0}{I}\right) = -\log T \quad 10$$

The Beer-Lambert's law therefore becomes:

$$A = \varepsilon c b \quad 11$$

3.3.3 Principle of A280 measurement and Determination of protein concentration

The protein A280 method is applicable to purified proteins that absorb light at 280 nm. The method uses the A280 absorbance value in combination with either the mass extinction coefficient or the molar extinction coefficient to calculate the concentration. The advantage of A280 measurement is that the concentration determination does not require the generation of a standard curve.

3.4 Microscopy

3.4.1 Basic of light microscopy

Light microscopy follows the physical laws that defines how light interacts with objects. Light travelling from one medium to another with different refractive index will change direction and velocity following Snell's law of refraction, where n_i is the refractive index of the respective medium and, θ_1 is the angle of incidence, and θ_2 is the angle of refraction.

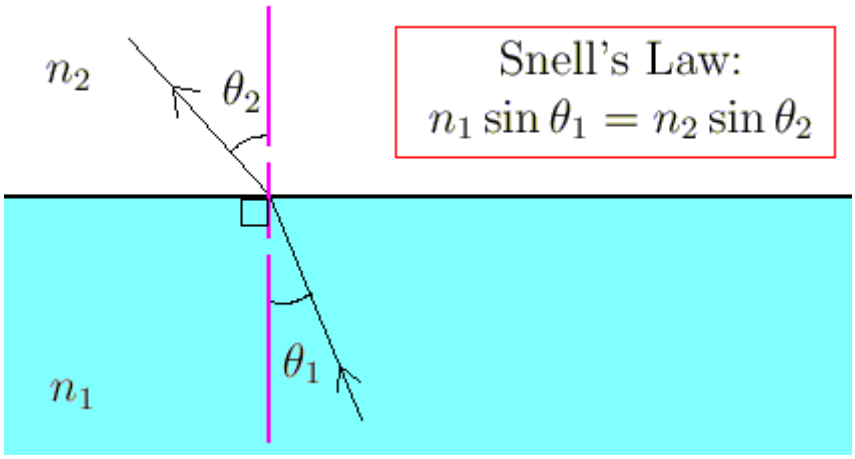

Figure 5 [21]. Principle of Snell's law.

Diffraction describes how light bends when it meets the edges of an object. An optical system can take advantage of these basic principles to form an image using lenses. Refraction and diffraction determine what form the image will take. The point spread function (PSF) gives information about the ability of an imaging system to generate the image of a point source of light [22]. The PSF defines the degree of blurring given by the system, after the light refracts and diffracts through the optical path. The numerical aperture, which decides the widest angle the can be collected by the lens, defines the size of the PSF. The wider the numerical aperture the smaller the PFS which gives better resolution.

Light microscopy is an important instrument in biology. The microscope must complete three tasks: magnify the image of the specimen, separate the details in the image (resolution), and make the details visible and construction.

3.4.1 Fluorescence Microscopy

A fluorescence microscope refers to any microscope that uses fluorescence and phosphorescence to generate images, whether it is a simpler one like an epifluorescence microscope, or a more complicated one such as confocal microscope, which utilizes optical sectioning to get better resolution [23]. The specimen is irradiated with a light of specific wavelength. The fluorophores absorb light and thereafter emit light of longer wavelengths. The excitation light is separated from weaker fluorescence. Typical components of a fluorescence microscope are a light

source, the excitation filter, the dichroic mirror (or dichroic beam splitter), and the emission filter.

In epi-fluorescence microscope (see Figure 6), light of a specific wavelength is produced by passing light from a light source through a wavelength selective exciter filter. The dichromatic mirror is tilted at a 45° angle with respect to the incoming excitation light and reflects this illumination at a 90° angle directly through the objective optical system and onto the specimen. Fluorescence emission produced by the illuminated specimen is gathered by the objective and because the wavelength of the emitted light is longer than the wavelength of excitation, it can pass through the dichromatic mirror and upward to the observation tubes or electronic detector.

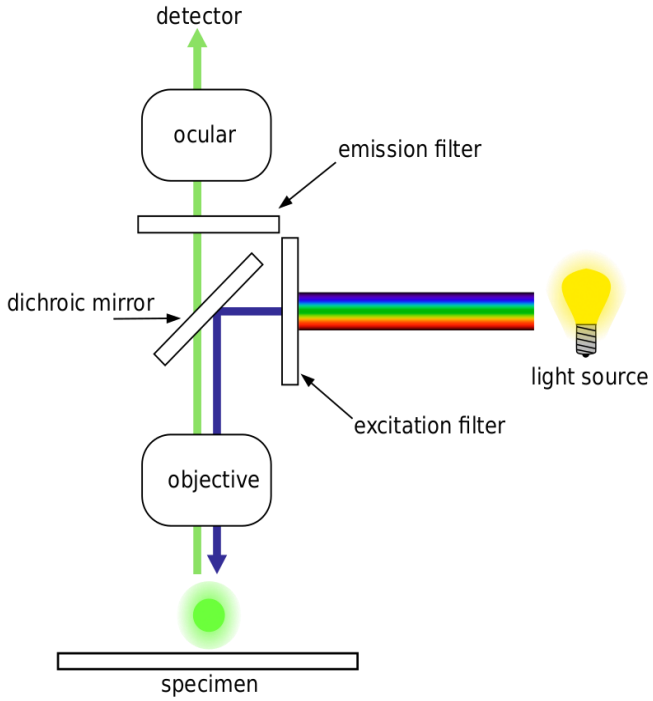

Figure 6 [43]. Graphical representation of the design of an epi-fluorescence microscope

3.4.2 Confocal Microscopy

A confocal microscope combines two principal ideas: point by point illumination of the sample and blocking of out of focus light [24]. Figure 7 shows the scheme of a confocal microscope. The excitation light (blue line) reflects off a dichroic mirror. From here, the light hits a pair of mirrors that scan the light in x and y. The light continues to pass through the microscope objective and excites the fluorescent sample. The emitted

(light green) light from the sample passes back through the objective and is descanned by the same mirrors that are used to scan the excitation light. The light then passes through the dichroic mirror through a pinhole placed in the conjugate focal (hence the name confocal) plane of the sample. The pinhole blocks all out-of-focus light. The light that passes through the pinhole is measured by a detector. Sharp and distinct image is achieved. At a time, only one point of the sample is observed. Multiple planes are scanned by the microscope by changing the focal point to reconstruct two-dimensional image. Thereafter, three-dimensional images are reconstructed by combining two-dimensional images at different depth.

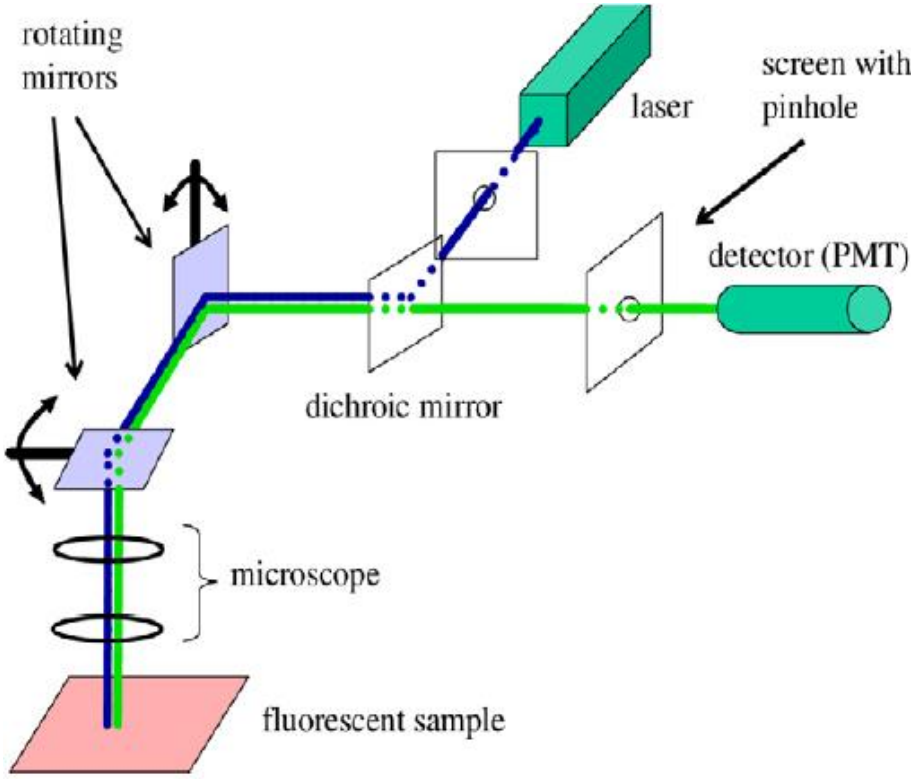

Figure 7 [24]. The scheme of confocal microscopy.

Chapter 4

4. Results and Discussion

Protein adsorption to polystyrene surface can be driven in many different such as Van der Waals forces, hydrogen bonding, electrostatic interactions and hydrophobic forces [3]. Interaction between a specific protein and a sorbent is generally influenced by several factors such as pH, ionic strength, temperature, properties of sorbent as well as the properties of the solvent [25] [26]. As a model system I have studied binding of SA-AF 488 to hydrophobic PSMs by passive adsorption and to hydrophilic PSMs by covalent coupling. To achieve this goal, pictures of randomly chosen SA-coated PSMs were taken using confocal microscopy and then analysed with the program ImageJ. The area, the integrated intensity and the mean gray value of each particle was determined. Thereafter, the Corrected Total Cell Fluorescence (CTCF) was calculated using the formula in Eq.17

CTCF= Integrated Density – (Area × Mean Fluorescence of Background readings) **12**

A surface plot was also taken to investigate the quality and evenness of adsorption. The amount of protein adsorption was estimated from the variation in free SA-AF 488 concentration before and after adsorption, calculated from the solution adsorption at 280 nm, using Nanodrop 2000.

4. Passive adsorption

Passive adsorption of proteins to PS surfaces has been argued to be driven by hydrophobic forces [4] [3] [5]. Because it is simple and flexible to perform passive adsorption, it is widely used. Here we want to study if the protein can effectively attach to PSMs. Figure 8 shows adsorption of streptavidin onto unmodified polystyrene beads with diameter 6 µm at two different pH values. When 1 µL of SA-AF488 was added to 100 µL of 10% w/v 6 µm-Polystyrene beads using 0.1M MES pH 5 as adsorption buffer and stored in 10mM HEPES pH 7. 4, it can easily be observed that the coating was not

uniform (Figure 8A). This is also shown with the plot profiles in Figure 9 (a graph of the intensities along a line or rectangular selection). The confocal pictures in Figure 11 were taken at the same settings and are thus comparable. For the PSMs that are marked number 1 in Figure 8, the plot profiles are shown as orange line in Figure 9. A high peak appears in all plot profiles of these PSMs which imply the proteins are bound mostly there. The plot profile should not have a high peak because if the proteins are bound evenly, the plot profile should look like the blue line. The blue lines demonstrate the intensity of the beads that are marked as number 2. The plot profiles of relatively uniform beads contain smaller variations i.e. they are closer to a straight line. The difference in CTCF indicates that proteins are not bounded equally strong to every microsphere.

If a protein is structurally stable, its orientation can be described as 'side-on' and 'end-on' orientation which is related to how the protein is attached to the surface with its long and short axis, respectively [27] [28] [29]. The layer thickness of protein monolayer in saturation state is higher in the 'end-on' oriented proteins than the 'side-on' oriented proteins [30] [31]. After a certain time, the loosely bound proteins in the end-on orientation start to desorb from the surface. This might be one reason for the difference in intensities of the SA-PSM microspheres. Another explanation can be the cooperative effect. It has been observed that the complex electrostatic field in the edge of adsorbed proteins induces a kind of electrostatic self-assembly which enhance the adsorption [32] [33]. Hence, the approaching proteins are preferred to adsorb in the close neighbourhood of pre-adsorbed proteins.

The pH controls charge of the proteins. When the pH is equal to the isoelectric point (IEP) of the protein, the negative and positive charges are in balance which leads to a net neutral molecule. Electrostatic repulsion between proteins is at a minimum when the pH of the adsorption buffer is equal IEP allowing a higher packing density on the surface [34]. This can be observed in the values of CTCF and the amount of bound protein (see Table 1). The proteins are always absorbed more when the adsorptions are performed in MES pH 5 which is close to the IEP of SA-AF 488. The amount of absorbed protein is 0.96 µg (sample 1) versus 0.80 µg (sample 3) for the SA-PSMs stored in HEPES, and 0.97 µg (sample 2) versus 0.94 µg (sample 4) for the SA-PSMs

stored in MES. While adsorption buffer should benefits the adsorption to give maximal efficiency. The storage buffer should reduce nonspecific binding and self-agrregation of the microspheres. Thus, storage buffer will not contribute to adsorption process but it will prevent bound proteins from desorption and keep protein-PS conjugate from aggregation. For all four samples, there were no aggregations. The CTCF value indicates how strong the binding is as well as the stability of PSM-microspheres. Hence, the higher CTCF, the stronger binding becomes. The CTCF is 787 (sample 1) vs 1817 (sample 2) for the beads prepared in MES buffer; 1021 (sample 3) vs 1138 (sample 4) for the microspheres prepared in HEPES pH7.4.

Table 1. The adsorption buffer controls the efficiency of adsorption while the storage buffer controls the stability of the microspheres after the adsorption. Column CTCF shows the average Corrected Total Cell Fluorescence that were determined by ImageJ. The amount of bound protein was determined using Nanodrop and Beer-Lambert's law. The added amount of SA-AF 488 is 1 µg. From the volume, diameter, and the density of PS suspension, the number of the microspheres as well as the surface area of one microsphere can be calculated. Total surface area of microparticle is number of PS multiplies with the the surface area of one PS. The number of bound proteins is determined from the weight of bound proteins. Total surface of bound protein is the number of proteins multiplies with surface are of one protein which is 25 nm². Datails code source for calculation is shown in Appendix.

	Adsorption buffer/Storage buffer	$V_{polystyrene}$ (µL)	Total surface area of PSM (µm²)	$V_{protein}$ (µL)	CTCF	Bound protein (µg)	Total surface area of bound SA (µm²)
1	MES/HEPES	100	9.52×10^{8}	1	787	0.96	2.74×10^{8}
2	MES/MES	100	9.52×10^{8}	1	1817	0.97	$2.77e\times10^{8}$
3	HEPES/HEPES	50	4.76×10^{8}	1	1021	0.803	2.29×10^{8}
4	HEPES/MES	50	4.76×10^{8}	1	1138	0.94	2.68×10^{8}

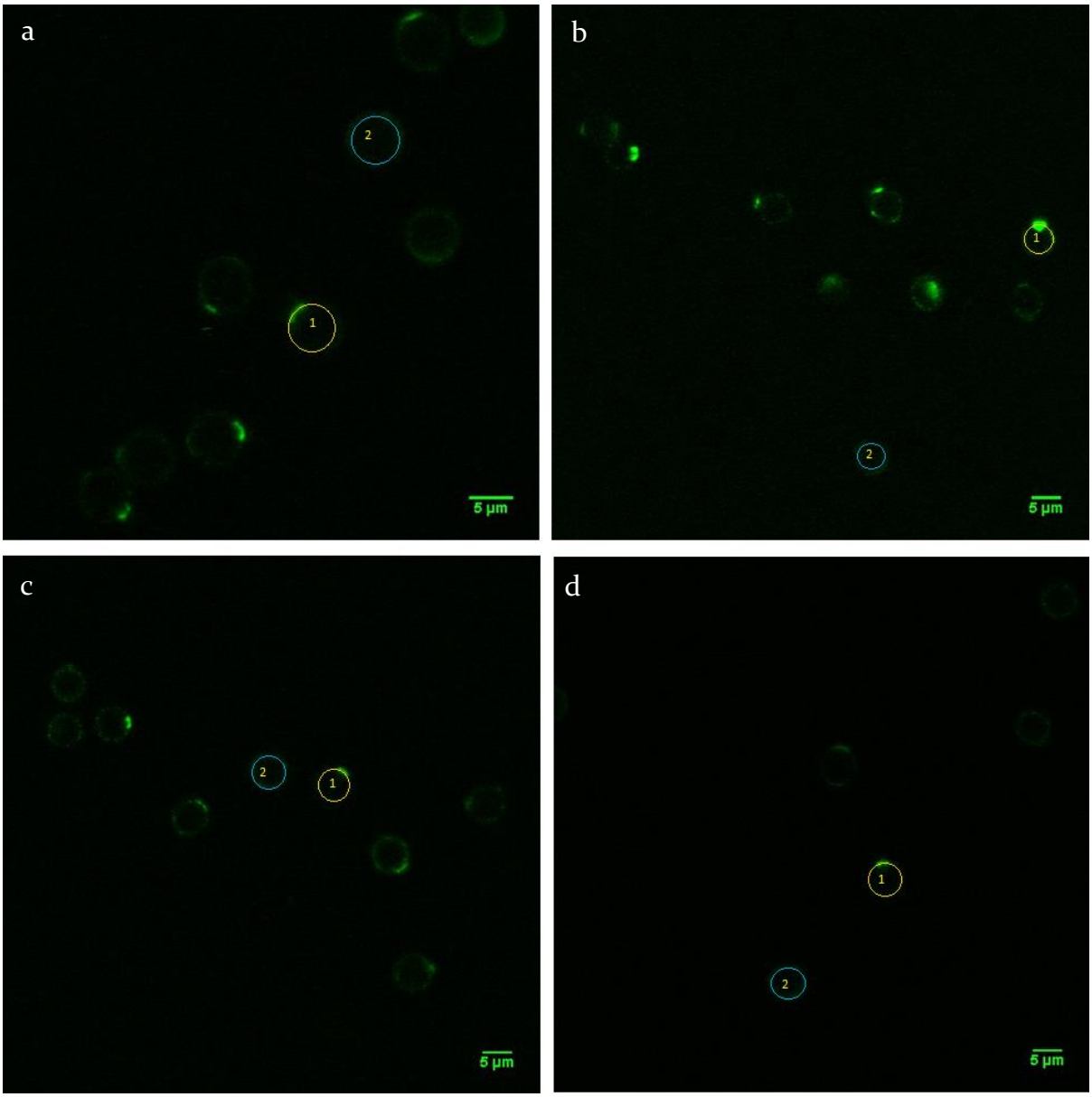

Figure 8. A) 100 µL of 10% w/v PMSs of size 6 µm was coupled with 1 µL of SA-AF 488. The adsorption buffer was 0.1M MES pH 5 and the storage buffer was 10mM HEPES pH 7.4. B) 100 µL of 10% w/v PMSs of size 6 µm was coupled with 1 µL of SA-AF 488. The adsorption buffer and the storage buffer was 0.1M MES pH 5. C) 50 µL of 10% w/v PMSs of size 6 µm was coupled with 1 µL of SA-AF 488. The adsorption buffer was 10mM HEPES pH 7.4 and the storage buffer was 0.1M MES pH 5. D) 50 µL of 10% w/v PSMs of size 6 µm was coupled with 1 µL of SA-AF 488. The adsorption buffer and the storage buffer was 10mM HEPES pH 7.4.

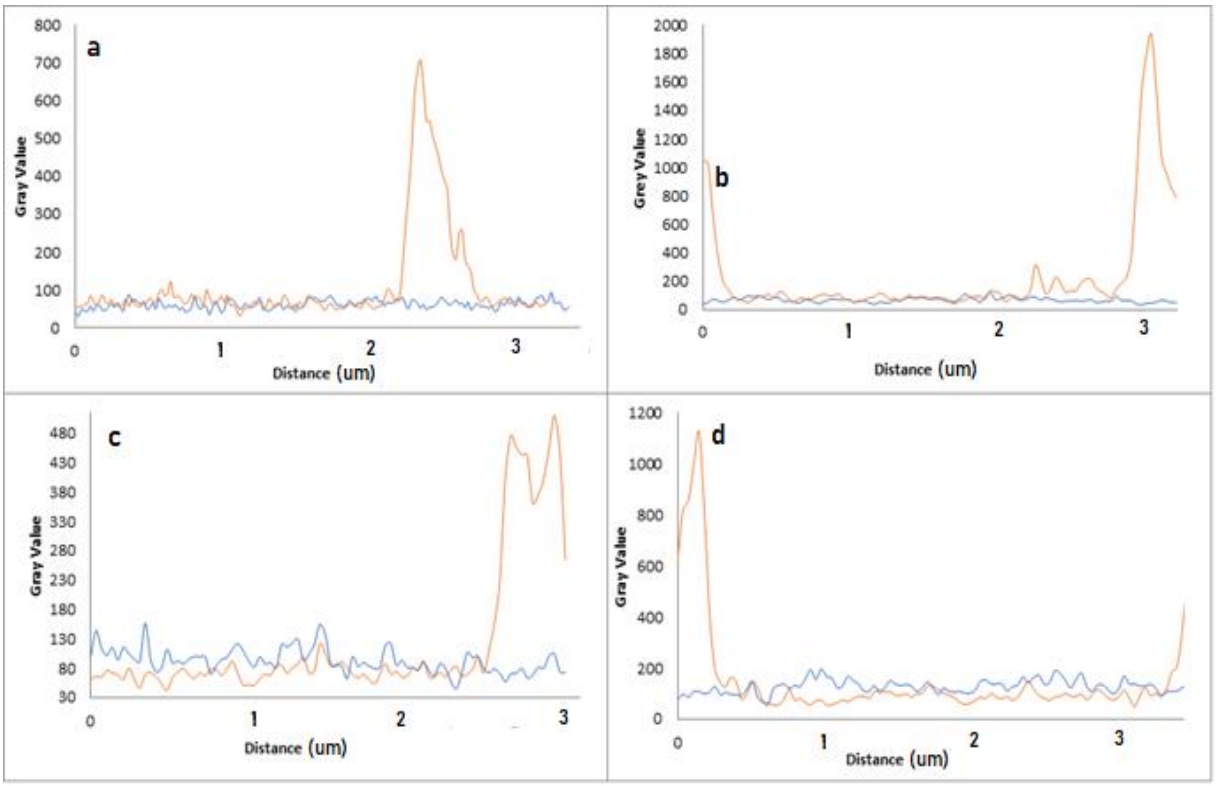

Figure 9. Plot profiles of two different PSMs that are marked with number 1 and 2 in Figure 11. The plot profile was taken around the PSM using ImageJ and shown in two different colors, orange for PSMs that are marked with number 1 and blue for PSMs marked with number 2. A) Samples prepared in 0.1M MES pH5 and stored in 10mM HEPES pH 7.4. B) Samples prepared and stored in in 0.1M MES pH5. C) Samples prepared in 10mM HEPES pH 7.4 and stored in 0.1M MES pH5. D) Samples prepared and stored in in 10mM HEPES pH 7.4.

4.2 Covalent coupling

PSMs show an important deficiency: proteins that are attached onto the particles by physical adsorption will slowly desorb during storage. They can also be denaturated due to the structural rearrangements that occur along the adsorption process [35, 36, 37, 38, 39]. Covalent coupling results in better reproducibility and more stable surface because desorption of protein is minimized. The PSMs must be functionalized to make their surface enable to covalent crosslinking with proteins. Reactive surface group such as amino and carboxyl are used to modify the surface of the microparticles.

4.2.1 Amino-modified PSMs (PSM-NH2)

Microparticles with smaller size give larger surface to volume ratio. PS-NH2 microspheres of size 1 µm were used for this study. The number of PSM-NH2 microspheres in 5 µL is 9.1×10^{8} and the total surface area of the beads is 2.86×10^{9} µm². If we assume the surface area of each streptavidin is 25 nm², the number of proteins in 5 µL of 1mg/ml SA-AF488 is 5.7×10^{13} and the total surface area of the proteins is 1.43×10^{9} µm². From this calculation, we see that the amount of proteins is only enough to cover half of PS-NH2 microspheres 'surface area even if the binding is 100%, but I still wanted to investigate if a good coupling can be achieved even at low amount of proteins.

A blocker can be added to the storage buffer to block the exposed hydrophobic surfaces of microspheres. This will reduce nonspecific coupling and self-aggregation of microspheres. β-casein is a milk- based protein, often used to passivate surfaces, which is made of biotin. This should be avoided if the working system contains biotin to prevent interference. β-casein can bind to SA and causes clumping. To verify if β-casein is unsuitable blocker for this coupling, 1 mg/ml β-casein in PBS was used as storage buffer.

5 µL of 1 mg/mL Streptavidin was coupled to 5 µL of 10% w/v amino-polystyrene microsphere of size 1 µm. The concentration of unbound protein could not be determined by the Nanodrop. Since the lowest concentration that can be detected with the Nanodrop is 0.002 mg/mL it can be assumed that essentially all of proteins were

bound to the PS-NH_2 microspheres and therefore half of PS-NH_2 microspheres′ surface area was covered by the proteins. The volume of protein was next increased to 10 µL and the volume of polystyrene was keep at 5 µL. The total surface area of protein is now 2.85×10^9 μm^2 so it should be able to get the microspheres covered. The activation time was also varied at this concentration (Sample 2 was activated overnight and sample 3 was activated under two hours). The amount of bound protein is 8.1 and 8.4 for the microspheres that were activated under two hours and overnight, respectively. The percent of surface area that are covered by proteins is 80 and 84%, respectively (

Table 2). The difference is not big, so it can be said that the activation time does not affect the quality of the coupling. However, extensive clustering of the PSMs was observed (Figure 10), which I attribute to β-casein binding to SA on the microspheres.

Storage buffer	$V_{polystyrene}$ (µL)	$V_{protein}$ (µL)	Bound protein (µg)	Total surface area of bound SA (µm²)	Percent of covered surface (%)
β-casein in PBS	5	5	5	1.43×10^9	50
β-casein in PBS	5	10	8.4	2.39×10^9	84
β-casein in PBS	5	10	8.1	2.30×10^9	80
PBS	5	8	3.6	1.07×10^9	37
Glycine in PBS	5	8	3.7	1.06×10^9	37

The coated surface decreased significantly when the amount of protein decreased to 8 µL and PBS as well as 1mg/mL glycine in PBS was used as storage buffer. The storage buffer was also changed to PBS and 1 mg/mL glycine in PBS to examine if the number of clusters was minimized. The coupling was not able to be observed with confocal microscope. Therefore, conclusion about the effect of different storage buffers cannot be made in this case. However, not using β-casein as the storage buffer was observed to reduce the clustering for carboxylated PSMs as described below

Table 2. The used volume of 10% w/v PSM-NH_2 and the volume of added protein. The pH is 7.4 for all three samples. The concentration of β-casein and glycine in PBS is 1 mg/mL. The last three samples were activated under two hours. The total surface area of the beads is 2.86×10^9 µm².

Storage buffer	$V_{polystyrene}$ (µL)	$V_{protein}$ (µL)	Bound protein (µg)	Total surface area of bound SA (µm²)	Percent of covered surface (%)
β-casein in PBS	5	5	5	1.43×10^9	50
β-casein in PBS	5	10	8.4	2.39×10^9	84
β-casein in PBS	5	10	8.1	2.30×10^9	80
PBS	5	8	3.6	1.07×10^9	37
Glycine in PBS	5	8	3.7	1.06×10^9	37

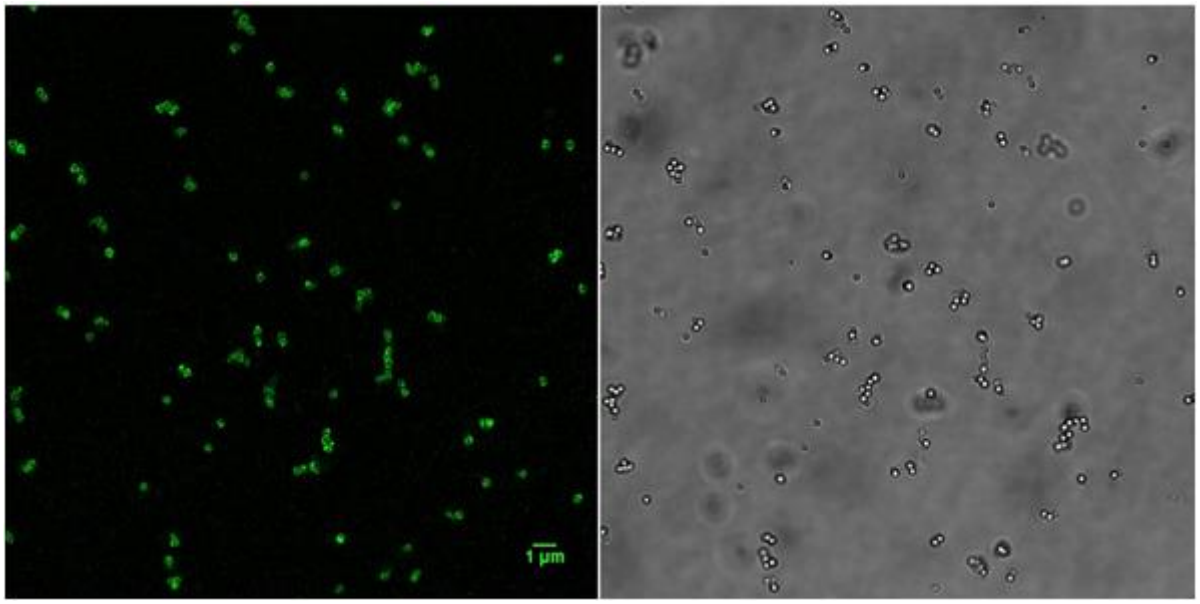

Figure 10. 10 µL of 1 mg/mL Streptavidin was coupled to 5 µL of 10% w/v of 1 µm amino-polystyrene microspheres. The microspheres were activated under two hours, and the storage buffer was 1 mg/mL β-casein in PBS pH 7.4.

4.2.2 Carboxylate -modified PSM (PSM-COOH)

According to the calculations in the last section, 10 µL of 1 mg/mL SA-AF 488 is a suitable amount to couple to 5 µL of PS-COOH beads as the total surface area of the microspheres is 2.86×10^9 µm² and the total surface area of the protein is 2.85×10^9 µm². When 10 µL of 1 mg/mL Streptavidin was coupled to 5 µL of PSM-COOH microspheres and the storage buffer was 1 mg/mL β-casein in PBS pH 7.4, a good coupling occurred although there were some clusters (Figure 11 and Table 3). Plot profiles of sample 1, 3 and 4 were taken by measuring the grey value around the coated PSM microsphere (Figure 14). Unlike the plot profiles of the microspheres obtained by passive adsorption, the plot profiles of coated PS-COOH microsphere show only minor fluctuations of the gray values instead of high peak which implies evenly coated PS-COOH microspheres.

Because microsphere clusters could be observed, especially in the last sample, two other storage buffers were tested: 1 mg/mL glycine in PBS pH 7.4 and PBS pH 7.4, and the amount of added protein was also reduced to 8 µL to test if less clusters would appear. For this protein volume, when the coated PS-COOH microspheres were stored in 1 mg/mL β-casein in PBS pH 7.4, even more clusters were observed (Figure 12). This time, the coated microspheres also showed lower intensity. The number of clusters decreased significantly when the coated PSM-COOH microspheres were store in PBS pH 7.4 or in 1 mg/mL glycine in PBS pH 7.4 (see Figure 13). Compared to the two samples of 8 µL of 1 mg/mL SA-AF 488 coupled to 5 µL of 10% w/v PS-NH2 microspheres that were also stored in PBS and 1 mg/mL glycine in PBS pH 7.4, the coupling of streptavidin onto PS-COOH microspheres with the same parameters was better as there are more proteins bound to PS-COOH microspheres (4 versus 2.6 µg for the microspheres stored in PBS and 4.6 versus 2.7 µg for the microspheres that stored in 1 mg/mL glycine in PBS). This is in line with previous reports [40] [41]. The reason why streptavidin binds more to PS-COOH is unknown.

Table 3. The volume of 10% w/v 1 µm- carboxylated PSMs that was used and the volume of added protein. CTCF of the microspheres was determined with confocal microscopy and the weight of bound protein was determined using Nanodrop. Sample 1 and 2 are store in 1 mg/mL β-casein. Sample 3 is stored in PBS and sample 4 is stored in 1 mg/mL glycine in PBS. The pH is 7.4 for all samples. The total surface area of the microspheres is 2.86×10^9 µm². For the last three samples, the amount of bound protein is similar but the CTCF values vary enormously. It could depend on the pictures were taken using different settings.

Storage buffer	$V_{polystyrene}$(µL)	$V_{protein}$ (µL)	CTCF	Bound protein (µg)	Total surface area of bound SA (µm²)	Percent of covered surface (%)
β-casein in PBS	5	10	2707	7.5	2.32×10^9	81
β-casein in PBS	5	8	389	4.6	1.32×10^9	46
PBS	5	8	1962	4.0	1.14×10^9	39
Glycine in PBS	5	8	3040	4.6	1.30×10^9	45

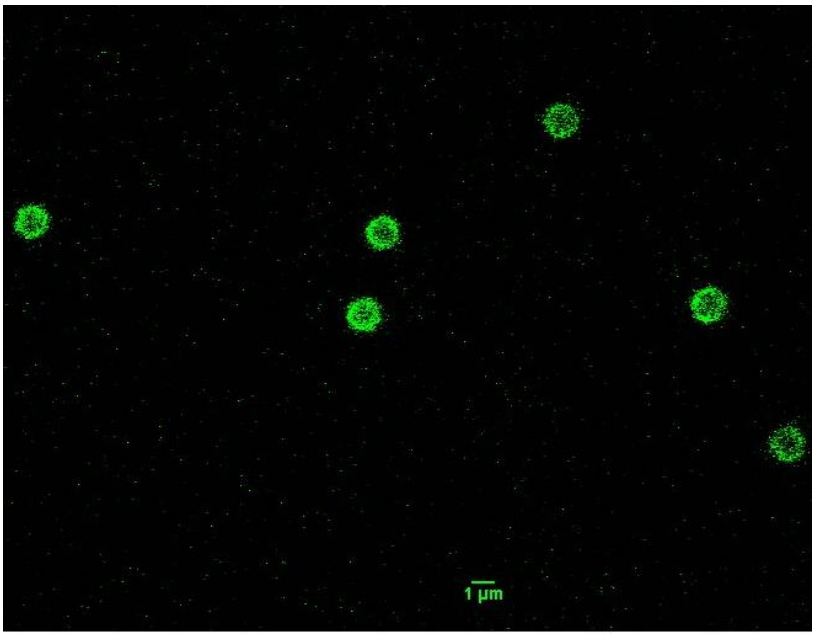

Figure 11. 10 µL of 1 mg/mL Streptavidin was coupled to 5 µL of 10% w/v of 1 µm carboxylated-polystyrene beads. The storage buffer was 1 mg/mL β-casein in PBS pH 7.4.

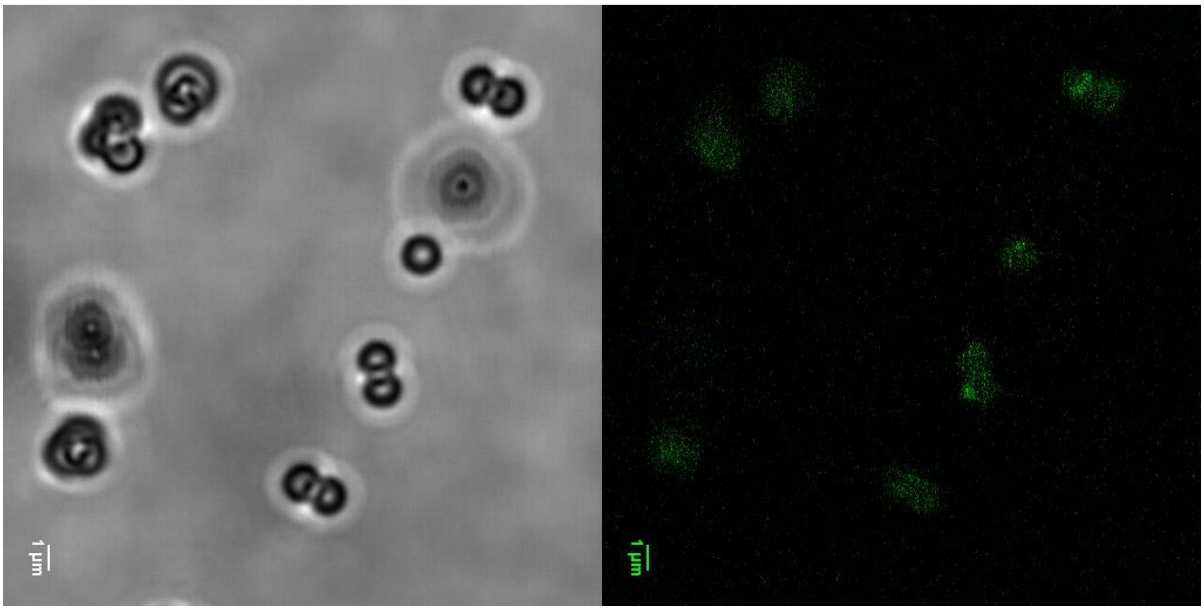

Figure 12. 8 µL of 1 mg/mL Streptavidin was coupled to 5 µL of 10% w/v of 1 µm carboxylated -polystyrene microspheres. The storage buffer was 1 mg/mL β-casein in PBS pH 7.4.

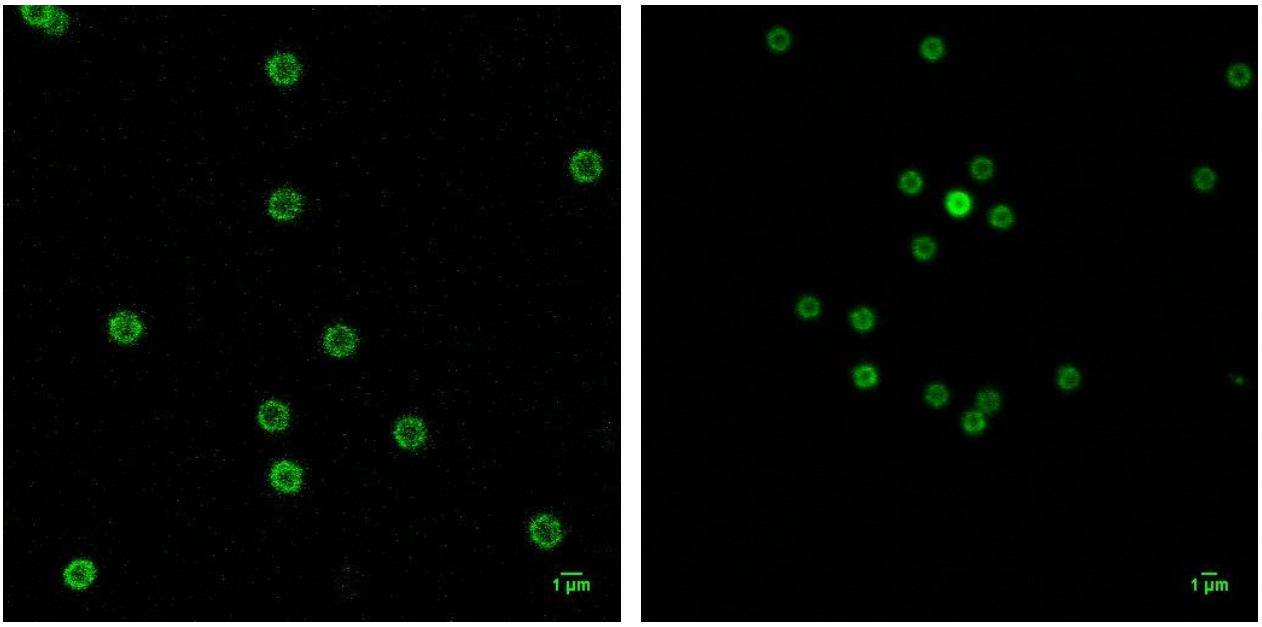

Figure 13. (Left) 8 µL of 1 mg/mL Streptavidin was coupled to 5 µL of 10% w/v of 1 µm PSM-COOH microspheres.SA-PSM microspheres were stored PBS pH 7.4. (Right) 8 µL of 1 mg/mL Streptavidin was coupled to 5 µL of 10% w/v of 1 µm PSM-COOH microspheres. SA-PSM microspheres were stored in 1mg/mL glycine in PBS pH 7.4.

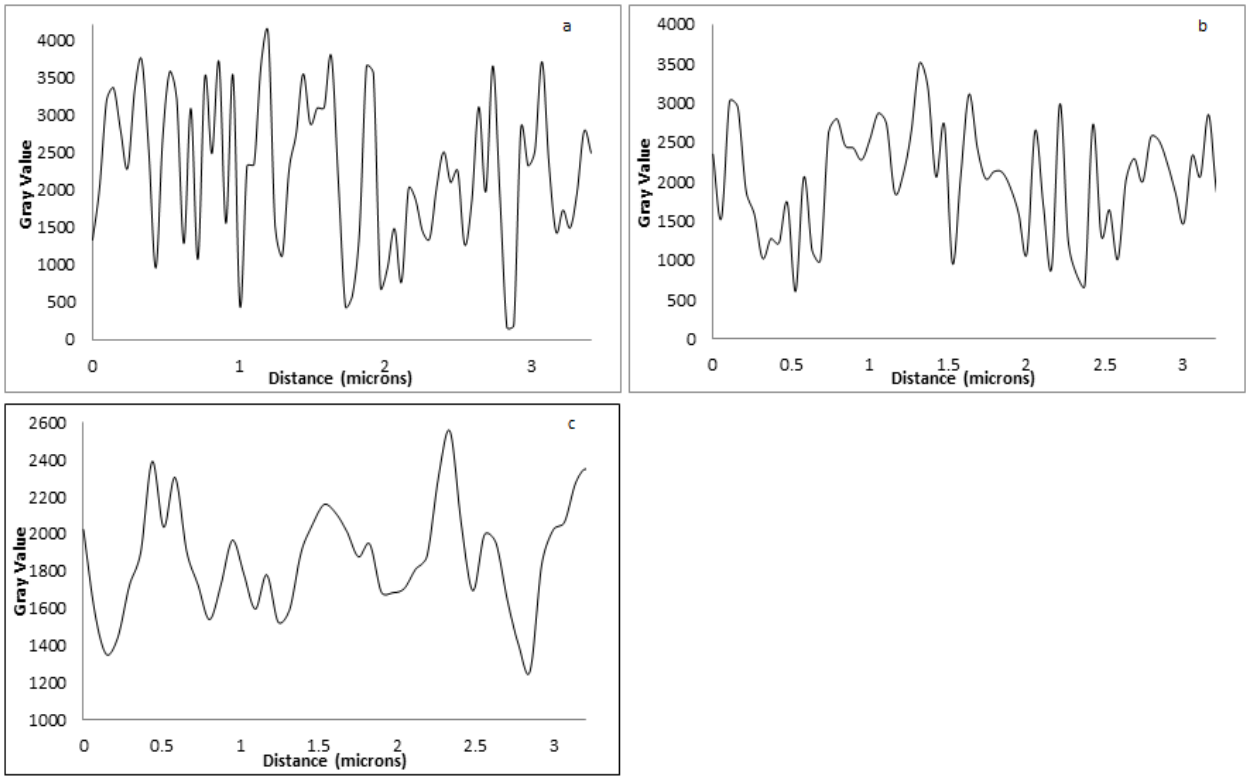

Figure 14. . Plot profiles for A) 10 µL of SA-AF 488 coupled to 5 µL carboxylated-polystyrene microspheres of size 1 µm. 1 mg/mL β-casein was used as blocker. B) 8 µL of SA-AF 488 coupled to 5 µL carboxylated-polystyrene microspheres. No blocker was used. C) 8 µL of SA-AF 488 coupled to 5 µL carboxylated-polystyrene microspheres of size 1 µm. 1 mg/mL glycine was used as blocker. Grey value was measured around the microsphere.

Chapter 5

5. Conclusion

5.1 Conclusion

The protein adsorption on nonfunctionalized polystyrene microparticles as well as functionalized polystyrene microparticles with different functional groups was investigated qualitatively and quantitatively using Nanodrop and confocal microscope. For passive adsorption of proteins on nonfunctionalized microparticles, the maximum adsorption is obtained at pH 5, which is in the neighbourhood of the IEP of the protein. Although the passive adsorption was simple to perform, and proteins were adsorbed onto the surface of PSMs with high density binding is not uneven. A more even binding of streptavidin to the PSMs was achieved with covalent coupling. It was shown that surface bearing acidic functional groups such as PSM-COOH is more favourable for covalent coupling the studied protein in this work than the surface with basic functional groups (PS-NH_2). The differences in protein adsorption onto various surfaces as presented here can be possibly utilized for antibody labelling.

5.2 Future work

The passive adsorption of protein onto polystyrene microspheres was not uniform and there were clumping of proteins on the spheres. This is possibly due to the low amount of protein, which could be increase (or the PSMs concentration decreased).

It was also found that measuring the protein concentration using Protein A280 mode was not always good regarding sensitivity and accuracy. Another method to measure the protein concentration is to measure absorbance at 228.5 nm and 234.5 nm. Protein concentration is then determined according to formula: c (mg/mL) = (A228.5 - A234.5)/ (extinction coefficient of Streptavidin × path length) [42].

Chapter 6

6. Acknowledgements

I would first like to thank Docent Peter Jönsson and Postdoc Mohammad Arif Kamal, my research supervisors, for their patient guidance, enthusiastic encouragement, and useful critiques of this research work. The door to their offices were always open whenever I ran into a trouble spot or had a question about my research or writing. They consistently allowed this paper to be my own work but navigated me in the right the direction whenever they thought I needed it.

I would also like to extend my thanks to Helena Persson, Maria Södergren, and Christopher Ward for their help under my time at Physical Chemistry department.

I would also like to acknowledge Professor Viveka Alfredsson as the examiner of this thesis.

References

[1] S. Kim, C. Kim, Y. Choi and M. Jung, *Polymer Bulletin* , no. 62, pp. 23-32, 2009.

[2] X. Hou, B. Liu, X. Dang, B. Zhang and J. Yab, *J Biomed Mater Res A,* p. 208, 2006.

[3] S. D and F. S, *Journal of Colloid and Interface Science,* vol. 221, no. 25, 2000.

[4] G.-G. F, M.-R. A and H.-A. R, *Colloid Polymer Science,* vol. 272, no. 352, 1994.

[5] H.-A. R. Vinuesa JBO, *J Biomater. Sci. Polymer Edn,* vol. 6(3), no. 269, 1994.

[6] H. Sun and N. Hu, *Biophys Chem* , no. 110, p. 297, 2004.

[7] V. Gonzalez, M. Chernova and G. Meira, *J Mater Sci: Mater Med,* vol. 2, no. 19, p. 777, 2006.

[8] "Latex Bead Technical Overview," Thermofisher Scientific, [Online]. Available: https://www.thermofisher.com/sg/en/home/life-science/cell-analysis/qdots-microspheres-nanospheres/idc-surfactant-free-latex-beads/latex-bead-technical-overview.html.

[9] A. Annapragada, *Annual Review of Medicine,* no. 66, pp. 177-193, 2015.

[10] D. A. Richards, A.Maruani and V.Chudasama, *Chemical Science* , no. 8, p. 63, 2017.

[11] V. Shargh, H. Hondermarch and M.Liang, *NAnomedicine,* no. 3, pp. 381-394, 2011.

[12] R. KOntermann, *Curr. Opin. Mol. Ther.,* vol. 8, no. 39, 2006.

[13] Y.Wang, *NAnomedicine,* no. 3, pp. 475-483, 2008.

[14] Y.Ishikawa, Y.Katoh and H.Ohshima, "Cooloidal stability of aqueous polymeric dispersions:Effect of pH and salt concentration," *Colloidal and Surface*

B:Biointerfaces, vol. 43, pp. 53-58, 2005.

[15] Y.Ishikawa, Y.Katoh and H.Ohshima, "Colloidal stability of aqueous polymeric dispersions:Effect of pH and salt concentration," *Colloidal and Surface B:Biointerfaces,* vol. 43, pp. 53-58, 2005.

[16] G. Malescio, "Intermolecular potentials - Past, present,future," *Nature Materials,* vol. 2, 2003.

[17] S. O. Majekodunmi, "A review on Centrifugation on the Pharmaceutical Industry," *American Journal of Biomedical Engineering* , vol. 5, no. 2, pp. 67-78, 2015.

[18] T. Ford and J. Graham, An Introduction to Centrifugation, BIOS Scientific Publishers, 1991.

[19] D. Rickwood, Centrifugation: A practical approach, Oxford University Press , 1984.

[20] P. Atkins and J. d. Paula, Physical Chemistry, Oxford University Press, 2010.

[21] [Online]. Available: https://www.math.ubc.ca/~cass/courses/m309-01a/chu/Fundamentals/snell.htm.

[22] E. H. K. STELZER, "Contrast, resolution, pixelation, dynamic range and signal-to-noise ratio: fundamental limits to resolution influorescence light microscopy," *Journal of Microscopy,* vol. 189, p. 15–24, 1998.

[23] J. C. Stockert and A. Blázquez-Castro, Fluorescence Microscopy in Life Sciences, Bentham Science, 2017.

[24] V. Prasad, D. Semwogerere and E. R. Weeks, "Confocal microscopy of colloids," *JOURNAL OF PHYSICS: CONDENSED MATTER,* 2007.

[25] N. W, Surface Chemistry in Biomedical and Environmental Science, Springer, 2006.

[26] E. R, L. YEM, S. APG and G. TCJ, *J Immunol Methods ,* vol. 152, no. 191, 1992.

[27] K. M and C. U, *Biophys J,* vol. 88, p. 3536, 2005.

[28] N. S, B. F, A. C and N. P. Baron D, *Biophys ,* vol. 85, p. 1196, 2003.

[29] W. CF and S. MM, *Langmuir ,* vol. 103, p. 1190, 2002.

[30] L. JR, Z. XB and Y. M. C. Opin, *Colloid Interface Sci ,* vol. 12 , no. 9, p. , 2007.

[31] S. TJ, L. JR, T. RK and P. J, *Langmuir,* vol. 14, p. 438, 1998.

[32] B. V and R. J, *J Phys Chem B ,* vol. 101, p. 5465, 1997.

[33] V. E.N and D. P., *Langmuir,* vol. 20, p. 8699, 2000.

[34] D. S, C. JP, MonrozierLJ and Q. H, *Colloids Surf B,* vol. 70, p. 226, 2009.

[35] A. J.D. and V. Hlady, "Protein adsorption and materials biocompatibility: a tutorial review and suggested hypotheses," *Adv. Polym. Sci.,* vol. 79, pp. 1-63, 1991.

[36] J. Andrade and V. Hlady, "Vroman effects, techniques, and philosophies," *J Biomater. Sci. Polymer Edn,* vol. 3, pp. 161-172, 1991.

[37] T. Basinka and A. Slomkowski, "Attachment of horseradish peroxidase (HRP) onto the poly(styrene/acrolein) latexes and their derivatives with amino groups on the surface: activity of immobilized enzyme," *Coll. and Polym. Sci.,* vol. 273, pp. 431-438, 1995.

[38] C. Haynes and W. Norde, "Structures and stabilities of adsorbed proteins," *J.Coll. Interf. Sci.,* vol. 169, pp. 313-328, 1995.

[39] D. Han, K. Park, G. Ryu, U. Kim, B. Min and Y. Kim, *J. Biomed. Mater. Res.,* vol. 30, pp. 23-30, 1996.

[40] A. Gessner, A. Lieske, B. Paulke and R. H.Müller, "Functional groups on polystyrene model nanoparticles: Influence on protein adsorption," *Journal of Biomedical Materials Research Part A,* no. 3, p. 319–326, 2003.

[41] C. Loos, T. Syrovets, A.Musyanovych, V. Mailänder, G. U. N. Katharina Landfester2 and T. Simmet, "Functionalized polystyrene nanoparticles as a platform for studying bio–nano interactions," *Beilstein J. Nanotechnol.,* no. 5, p. 2403–2412, 2014.

[42] E. B., I. P. and W. J.H., "Spectrophotometric determination of protein concentration in cell extracts containing tRNA's and rRNA's," *Anal. Biochem. .,* no. 54, p. 454–463, 1973.

[43] "Wikipedia," [Online]. Available: https://en.wikipedia.org/wiki/Fluorescence_microscope#cite_note-3.

[44] [Online]. Available: https://discoveries-project.weebly.com/anton-van-leeuwenhoek.html.

Appendix

Source code

Calculations for Polystyrene microparticle

```
clear all
clc
% Concentration of the microsphere solution in % (wt/v)
disp('------------------------------------------------------------')
C_bs= input ('Enter the concentration of the microsphere solution in (wt/v): ');
% Concentration of the microsphere solution in ug/ul
C_bs= C_bs*10;
disp('------------------------------------------------------------')
% Volume of the microsphere solution in ul
v_bs= input ('Enter the volume of the microsphere solution used in ul: ');
disp('------------------------------------------------------------')
% Mass of the microspheres used in ug
m_bs=C_bs*v_bs;
% Density of the microsphere solution in ug/ul
 rho_b= input('Enter the density of the microshperes used in g/cc : ');
rho_b= rho_b*10^(3);
disp('------------------------------------------------------------')
% Diameter of each bead in mm
 d= input('Enter the diameter of the microsphere used in um: ');
d=d*10^(-3);
disp('------------------------------------------------------------')
% Volume of one bead im mm^3(=ul)
v_b= (4*pi/3)*(d/2)^(3);

% Total no of beads
disp('------------------------------------------------------------')
disp('Results for the Microspheres')
```

```
disp('-------------------------------------------------------------')
N_b=m_bs/(rho_b*v_b);
disp(['Total no of beads in the solution: ' num2str(N_b,'%2.4e')])
 disp('-------------------------------------------------------------')
% Total surface area of microspheres (mm^2)
As=N_b*(4*pi*(d/2)^2);
disp(['Total surface area in Sq mm: ' num2str(As,'%2.4e')])
disp('-------------------------------------------------------------')
% Total surface area of microspheres (um^2)
A_b=As*10^(6) ;
disp(['Total surface area in Sq um: ' num2str(A_b,'%2.4e')])
disp('-------------------------------------------------------------')
```

Calculations for Streptavidin

```
 % Volume of added protein in uL
disp('-------------------------------------------------------------')
V_p= input('Enter the added volume of protein in uL: ');
V_p= V_p*10^(-3); %volume in mL
% Concentration of protein (mg/mL)
disp('-------------------------------------------------------------')
C_p= input('Enter the Concentration of protein in mg/mL: ');
 % Molecular weight of protein
disp('-------------------------------------------------------------')
M_p= input('Enter the Molecular weight of protein in kDa: ');
M_p= M_p*10^(9);
 %Surface area of one protein in square nm
disp('-------------------------------------------------------------')
Ap= input('Enter Surface area of one protein in square nm: ');
Ap=Ap*10^(-6); %Surface area in Sq um
 disp('-------------------------------------------------------------')
disp('Results for the Proteins')
disp('-------------------------------------------------------------')
```

```
% Weight of protein
m_p=(V_p*C_p)*10^3;
disp(['Weight of protein in microgram: ' num2str(m_p)])
disp('------------------------------------------------------------')
% Number of moles
n=m_p/M_p;
disp(['The Number of moles of protein: ' num2str(n,'%2.4e')])
disp('------------------------------------------------------------')
% Number of proteins
N_p=n*6.022*10^23;
disp(['The Number of proteins: ' num2str(N_p,'%2.4e')])
disp('------------------------------------------------------------')
% Total surface area of proteins
A_p=N_p*Ap;
disp(['Total surface area of Protein in Sq um: ' num2str(A_p,'%2.4e')])
disp('------------------------------------------------------------')
```